Ultrafast Rotational Anisotropy Measurements: Unidirectional Detection

Emily J. Brown, Igor Pastirk,† and Marcos Dantus*

Department of Chemistry and Center for Fundamental Materials Research, Michigan State University, East Lansing, Michigan 48824

Received: November 23, 1998; In Final Form: February 18, 1999

Unidirectional signal detection in time-resolved rotational anisotropy experiments has been known to affect the time zero and time infinity (persistent alignment) values because these measurements can overestimate the parallel or perpendicular components of the signal. Here we demonstrate that the well-known expression for obtaining the rotational anisotropy, a quantity that is typically calculated to measure the alignment, rotational energy, or rotational constants of molecules, is not applicable for some of the most common experimental configurations. We report new formulations that take into account different unidirectional detection schemes and the *f*-number of the collection optics. Femtosecond time-resolved anisotropy measurements on iodine vapor were obtained, with typical right-angle detection, to illustrate how the new expression corresponding to this configuration yields the expected time zero and time infinity values. Fits to the observed anisotropy are shown to provide quantitatively accurate results.

I. Introduction

Pump−probe spectroscopy using ultrafast lasers has advanced our understanding of molecular dynamics and chemical reactions in real time. Studies have been done on nonreactive systems where vibrational motion is observed as well as on reactive systems where bond dissociation and formation take place.[1−4] Here we concentrate on the angular motion of gas-phase molecules which reflects the rotations of the parent and daughter species. Polarized lasers are used in these measurements to follow the time evolution of the rotational alignment of the isolated molecules.[5−8] For reactive systems, one learns about the rotational impulse during the chemical reaction as well as the emergence of the final rotational population,[6,9] which in some cases can aid in the determination of a reaction mechanism.[10,11]

Theories for time-resolved rotational anisotropy measurements of isolated molecules have been developed using both quantum and classical mechanics.[6,9,12−14] Rotational anisotropy techniques are well established for the study of molecular structure as in rotational coherence spectroscopy.[15,16] The measurements are relatively simple and can yield quantitative information on the molecular structure of the molecule studied in addition to information on the overall rotational population. Given the multiple techniques available for ultrafast dynamics measurements such as laser-induced fluorescence, multiphoton ionization, and four-wave mixing, it is important to realize that the rotational anisotropy theory applies differently in each case. Changes in the formulation that include multiphoton pump or probe transitions have been recently discussed by Zhang et al.[11]

The ultrafast rotational anisotropy (URA) measurements of interest here are those that involve excitation by a linearly polarized laser pulse followed by probing after a variable time delay with a laser pulse polarized either parallel or perpendicular with respect to the excitation pulse (see Figure 1a). The initial population selected by the pump pulse is described by a $\cos^2\theta$ distribution where θ is the angle between the transition dipole and the pump laser polarization vector.[17] As the molecules rotate, the ability of the probe pulse to excite the molecules to another state varies and the fluorescence from this second state is monitored as a function of time delay between pump and probe pulses. The pure anisotropic component of the signal is obtained by subtraction of the parallel ($I_{||}$) and perpendicular ($I_{\perp}$) transients and division by the purely isotropic component of the signal, I_{iso}. On the basis of the work of Gordon,[18] the isotropic component can be obtained by the sum

$$I_{iso} = I_{||} + 2I_{\perp} \tag{1}$$

Thus, the URA can be obtained according to the formula[6,18]

$$r(t) = \frac{I_{||} - I_{\perp}}{I_{||} + 2I_{\perp}} \tag{2}$$

The simplicity of this formula is misleading. In fact, it applies only to a subset of the ultrafast dynamics detection techniques. Equation 2 is applicable only for measurements where eq 1 is true. Among these are experiments where the signal is the partial absorption of the probe, a common setup for liquid-phase experiments, or a measure of fluorescence depletion caused by the probe. In this study we explore the applicability of this formula to ultrafast measurements where the signal arises from probe laser-induced fluorescence (LIF). In particular, we explore the effect of unidirectional detection of the fluorescence signal taking into account the *f*-number of the collection optics. This experimental configuration is one of the most common in time-resolved gas-phase measurements.

II. Experimental Section

The experiments were conducted using a femtosecond laser system that produces 50 fs pulses centered at 622 nm with an average energy of 0.5 mJ per pulse (30 Hz repetition) as described in ref 19. Experiments were carried out with 622 nm pump, 311 nm probe, and 340 nm fluorescence detection (622/311(340)) or with 550 nm pump, 311 nm probe, and 340 nm

* To whom correspondence should be addressed. E-mail: dantus@cem.msu.edu.

† Affiliated with the Institute for Nuclear Sciences "VINCA", Belgrade, F. R. Yugoslavia.

10.1021/jp9845064 CCC: $18.00
Published on Web 04/03/1999

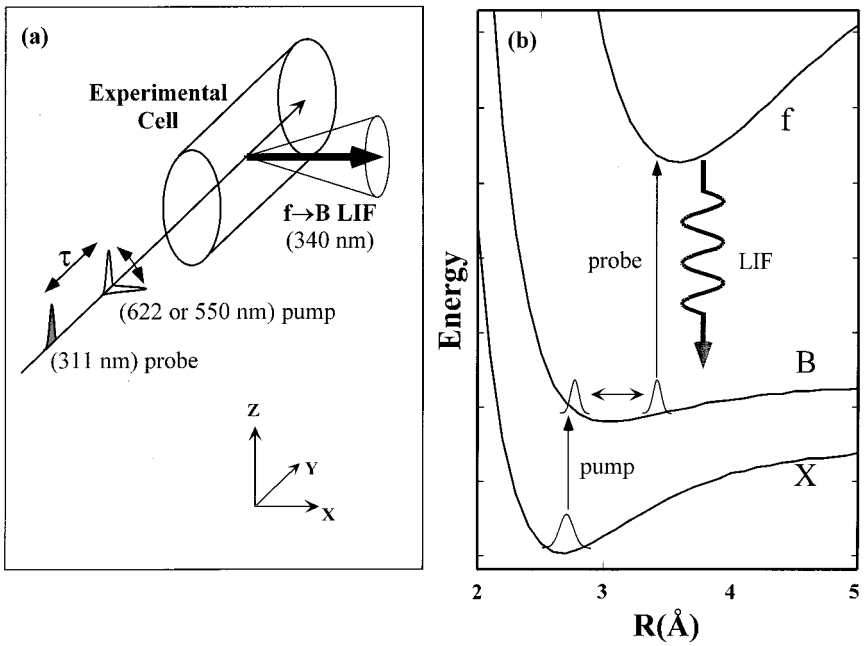

Figure 1. (a) Experimental setup. The probe beam remains polarized along the *Z* axis, while the pump beam can be rotated and is polarized along either the *Z* (||) or *X* (⊥) axis. LIF is collected perpendicular to the propagation of the lasers, along the *X* axis. (b) Potential-energy curves of I_2. The experiments measure the initial alignment and subsequent rotational dephasing of I_2 molecules that absorb a photon in a transition from the ground X state to the excited B state. The probe laser excites molecules in the B state to the E and f ion-pair states. The signal at 340 nm arises from LIF between the f and B states.

detection (550/311(340)). In the latter case, a frequency continuum was generated from the 622 nm beam and filtered to give 550 nm pulses for the pump. Saturation of spectroscopic transitions and detectors was prevented by attenuation of pump and probe beams to energies below 1 μJ per pulse. Unpolarized LIF in the 340 nm wavelength region was collected perpendicular to the laser beam propagation (see Figure 1); collection was restricted to $f = 3$. A quartz cell containing iodine was degassed (10^{-6} Torr) before being permanently sealed. Experiments were conducted at room temperature (21 °C) where the vapor pressure is 0.25 Torr. Figure 1b shows the relevant potential-energy curves for I_2 for these experiments.

Polarization measurements were performed with well-polarized beams. We measured polarization ratios (vertical:horizontal) after recombination of pump and probe lasers by the dichroic beam splitter. The polarization ratio of the probe laser, at 311 nm, was measured to be higher than 100:1. The polarization of this beam was kept perpendicular to the laser table for all experiments (*Z*-direction in Figure 1). The polarization of the pump laser (622 or 550 nm) was rotated parallel or perpendicular to the polarization of the probe laser with a zeroth-order half-wavelength plate. To ensure the highest polarization ratio in the pump beam, a calcite polarizer was used after the half-wavelength plate. With this setup, the polarization ratio of the pump beam was higher than we could experimentally determine $\sim 10^4$:1. Polarization ratios were also measured after the experimental cell to ascertain that no polarization scrambling occurred in the cell windows.

III. Theory

Rotational anisotropy is typically measured by obtaining transients for $I_{||}$ and $I_\perp$. The difference, $I_{||} - I_\perp$, contains isotropic contributions in addition to the time-dependent anisotropy.[18] Gordon noted that dividing the difference by the isotropic component of the signal as defined in eq 1 leads to a measurement that is independent of isotropic contributions and experimental parameters such as the relative signal intensity.

The dependence of URA measurements on the polarization of the pump−probe transitions has been discussed by Baskin and Zewail.[9] For the case when the fluorescence collection is proportional to the whole distribution (i.e., all-direction detection), one can consider the experimental signal for parallel and perpendicular pump−probe configurations to be of the form[9]

$$I_{||} = C \cdot A(t)(1 + 2\cos^2 \omega t) \text{ and} \tag{3a}$$

$$I_\perp = C \cdot A(t)(2 - \cos^2 \omega t) \tag{3b}$$

where $A(t)$ represents the time-dependent absorption probability of the probe beams (all isotropic), C is a proportionality constant that takes into account experimental conditions such as collection efficiency, and $\cos^2 \omega t$ represents the semiclassical time-dependent rotational dynamics where $\omega = 4\pi B_{\text{eff}} j$ and B_{eff} is the effective rotational constant of the molecule. For linear molecules, B_{eff} equals B. For clarity we refrain from discussing the rotation of asymmetric tops. Substitution of eqs 3a and 3b into eq 1 yields an expression in which the semiclassical time-dependent rotational dynamics terms ($\cos^2 \omega t$) cancel leaving I_{iso} proportional to $C \odot A(t)$. These terms cancel in eq 2. Thus, $r(t)$ depends only on the rotational population and the rotational constants of the molecule.

A central aspect for this analysis is that the experimental setup must satisfy eq 1, namely, that the denominator of eq 2 must be truly isotropic. This is the case for experiments where absorption of the probe laser is measured, as in many time-resolved condensed-phase experiments. Here we analyze one of the most common experimental setups used for gas-phase measurements and show that eq 1 is not fulfilled. While the effects of collection geometry have been noted before,[9] the implications have not been explored. The following treatment assumes large *f*-number collection; differences for small *f*-number collection are indicated later.

For unidirectional detection experiments, fluorescence collection favors signals from either parallel or perpendicular

probing configurations; thus, the signal is not proportional to the whole distribution. A common example is collecting probe-induced LIF at a right angle to the laser (e.g., *X*-direction) as shown in Figure 1. This point can be shown analytically using the following expressions to simulate the signals[9]

$$S_{\|X} = S_{\|Y} = \frac{2C}{105}(1 + 2\cos^2 \omega t) \tag{4a}$$

$$S_{\|Z} = \frac{C}{35}(1 + 2\cos^2 \omega t) \tag{4b}$$

$$S_{\perp Y} = \frac{C}{105}(3 - \cos^2 \omega t) \text{ and} \tag{4c}$$

$$S_{\perp X} = S_{\perp Z} = \frac{C}{210}(11 - 6\cos^2 \omega t) \tag{4d}$$

For these expressions, the polarization vector of the probe is fixed along the *Z* axis; the polarization vector of the pump is oriented along the *Z* or *X* axes for parallel or perpendicular measurements, respectively. The LIF signal arises from the components of the polarization dipole along each of the lab-fixed axes. For example, S_X corresponds to signal that is radiated by a dipole that is oriented along the *X* axis. Note that this radiation cannot be observed along the *X* axis itself. This is one of the reasons why unidirectional detection can over- or underestimate the ratio between parallel and perpendicular signals. Equations 4a−d are used to calculate $I_{\|}$ and $I_{\perp}$ for different detection directions. These expressions are shown in Table 1 in addition to other important equations and values in anisotropic measurements. Clearly the addition of $I_{\|}$ and $I_{\perp}$ for *X*-detection ($I = S_Y + S_Z$) according to eq 1 does not lead to the cancellation of the rotational term. Because the goal is to render the sum independent of molecular orientation, one can easily deduce the correct expression by substitution; these formulas are shown in Table 1. As shown in the table, the experimental $r(t)$ for *X*-detection can be calculated from the data using

$$r(t)_X = \frac{I_{\|} - I_{\perp}}{I_{\|} + \frac{5}{2}I_{\perp}} \tag{5}$$

So far the discussion has been limited to large *f*-number collection, where *f*-number is defined as the focal length divided by the diameter of the collection optic. However, it is important to recognize that most experimentalists maximize the collection efficiency by reducing the *f*-number of the collection optics. We calculated the relative contributions of eqs 4a−d as a function of *f* and again determined the proper expression for the $r(t)$ denominator by substitution. In the generalized rotational anisotropy formula

$$r(t) = \frac{I_{\|} - I_{\perp}}{I_{\|} + C(f)I_{\perp}} \tag{6}$$

the resulting coefficients $C(f)$ as a function of *f* for *X*, *Y*, and *Z* detection are

$$C_X(f) = \frac{5}{2} - \frac{7}{2(5 + 16\,f^2)} \tag{7a}$$

$$C_Y(f) = \frac{5}{3} + \frac{7}{12(1 + 6\,f^2)} \text{ and} \tag{7b}$$

$$C_Z(f) = 2 \tag{7c}$$

From eqs 7a−c, it is clear that for $f \geq 3$ the second term, containing the *f*-dependent correction, is negligible. Even for low *f* values, the deviation caused by the second term is small, 2% and 7% for $f = 2$ and 1, respectively, for *X*-detection. In general, physical constraints such as optical mounts, spatial filters, and spherical and chromatic aberrations make true $f = 1$ collection difficult. Therefore, for most URA measurements, no *f*-number correction is necessary.

The rotational anisotropy can be modeled semiclassically using[6,9]

$$r(t) = \frac{\sum_j P_j r_j(t)}{\sum_j P_j} \tag{8}$$

where P_j is the product state distribution of each *j* level. The rotational anisotropy is defined as a weighted sum of the individual rotational state anisotropies $r_j(t)$. Fits of the experimental $r(t)$ to eq 8 lead to the determination of the experimental rotational distributions. For the room-temperature measurements presented here, a Maxwell−Boltzmann distribution is assumed and a temperature is extracted to quantitate the accuracy of the measurement.

TABLE 1: Semiclassical Time-Resolved Anisotropy Expressions for Unidirectional Detection (Parallel Pump and Probe Transitions Assumed)[a] and Large *f*-Number Collection, $f \geq 3$

	A All-direction detection $I = S_X + S_Y + S_Z$	B *X*-detection $I = S_Y + S_Z$	C *Y*-detection $I = S_X + S_Z$	D *Z*-detection $I = S_X + S_Y$
$I_{\|}$	$\frac{C}{15}(2 + \cos(2\omega t))$	$\frac{C}{21}(2 + \cos(2\omega t))$	$\frac{C}{21}(2 + \cos(2\omega t))$	$\frac{4C}{105}(2 + \cos(2\omega t))$
$I_{\perp}$	$\frac{C}{15}\left(\frac{3}{2} - \frac{1}{2}\cos(2\omega t)\right)$	$\frac{C}{21}\left(\frac{13}{10} - \frac{2}{5}\cos(2\omega t)\right)$	$\frac{C}{21}\left(\frac{8}{5} - \frac{3}{5}\cos(2\omega t)\right)$	$\frac{4C}{105}\left(\frac{13}{8} - \frac{1}{2}\cos(2\omega t)\right)$
I_{iso}	$I_{\|} + 2I_{\perp}$	$I_{\|} + \frac{5}{2}I_{\perp}$	$I_{\|} + \frac{5}{3}I_{\perp}$	$I_{\|} + 2I_{\perp}$
$r(t)$	$\frac{I_{\|} - I_{\perp}}{I_{\|} + 2I_{\perp}}$	$\frac{I_{\|} - I_{\perp}}{I_{\|} + \frac{5}{2}I_{\perp}}$	$\frac{I_{\|} - I_{\perp}}{I_{\|} + \frac{5}{3}I_{\perp}}$	$\frac{I_{\|} - I_{\perp}}{I_{\|} + 2I_{\perp}}$
$r_j(t)$	$\frac{1}{10}(1 + 3\cos(2\omega t))$	$\frac{2}{15}(1 + 2\cos(2\omega t))$	$\frac{3}{35}(1 + 4\cos(2\omega t))$	$\frac{1}{14}(1 + 4\cos(2\omega t))$
$r(0)$	0.400	0.400	0.429	0.357
$r(\infty)$	0.100	0.133	0.086	0.071

[a] Corrections for multiphoton pump or probe measurements can be made by using the formulae in ref 11.

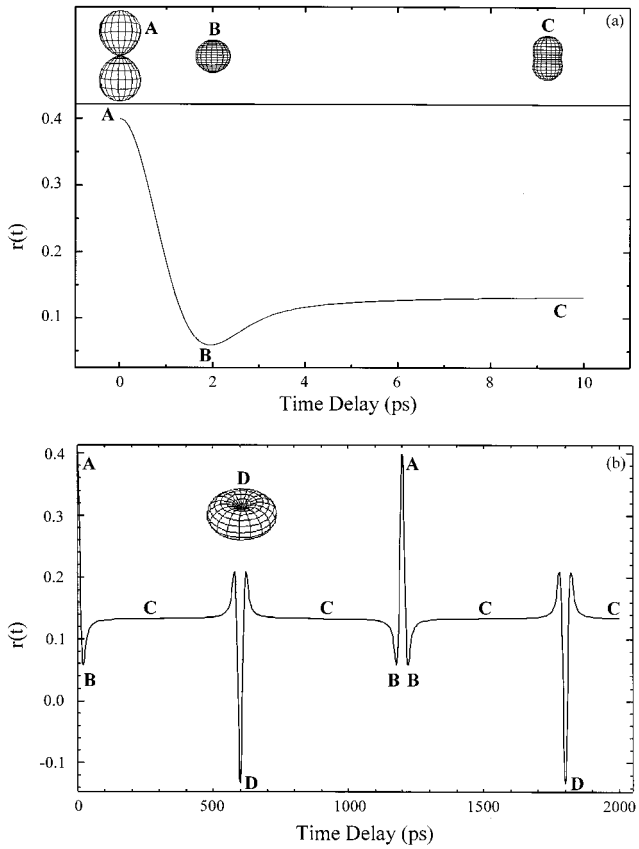

Figure 2. (a) Simulated rotational anisotropy graph for short time delays. The distribution quickly changes from the initial alignment (A) to an isotropic distribution (B) to a persistent alignment (C). Drawings of these distributions as viewed from the $X-Y$ plane are shown above the $r(t)$ graph. (b) Simulated rotational anisotropy graph at longer time delays. After the persistent alignment, a half-recurrence (D) develops. The drawing of this distribution is shown from a view out of the $X-Y$ plane so that the $\sin^2\theta$ shape (rotated around the Z axis) is evident. Each $r(t)$ is labeled with the distributions that occur as time evolves.

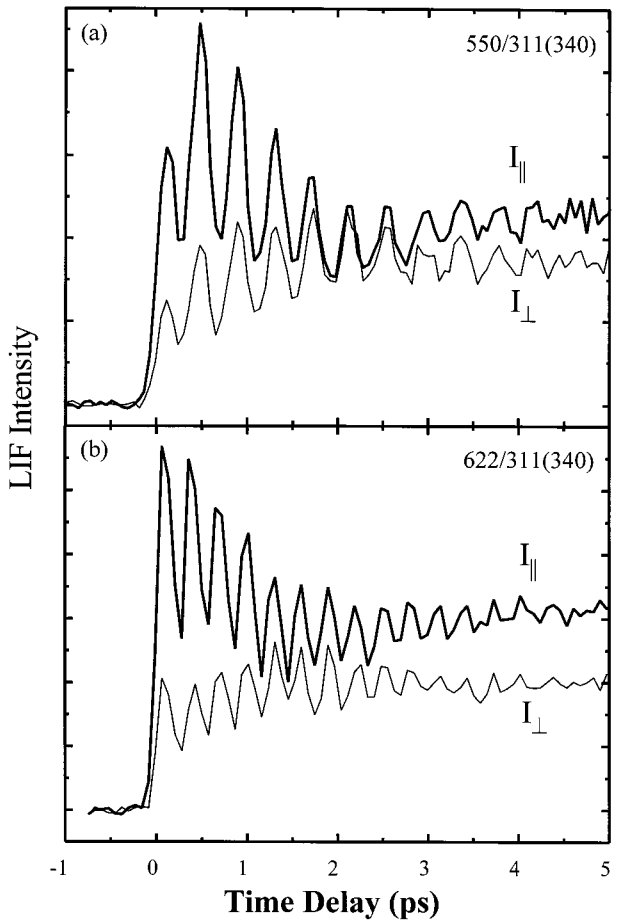

Figure 3. (a) Experimental $I_\parallel$ and $I_\perp$ transients for I_2 with 550/311-(340). (b) Experimental $I_\parallel$ and $I_\perp$ transient for I_2 with 622/311(340). Vibrations are clear in both sets of transients. Because different vibrational levels are reached on the anharmonic B state by the two excitation wavelengths, b shows faster vibrational dynamics than a. For the same reason, the rotational constants are also different for the two datasets, resulting in a slight difference in the rotational dynamics.

In Figure 2 we have shown snapshots of the distribution of molecular orientations, initially $\cos^2\theta$, at certain characteristic points on the $r(t)$ graph. These can be defined as (A) initial alignment or full-recurrence, (B) isotropic distribution, (C) persistent alignment, and (D) half-recurrence. This simulation assumes a single rotational constant and no centrifugal distortion. The time-dependent evolution has been simulated using semi-classical methods and a visualization of the evolution for a thermal rotational population can be found in ref 20.

In the absence of collisions, dilute gases, for example, molecules exhibit a persistent alignment (C) that favors parallel over perpendicular probing (parallel transitions assumed). As a consequence, fluorescence emission is anisotropic and the detection configuration influences the measurement. The loss of this persistent alignment as one enters the condensed phase is the subject of an elegant paper from Zewail's group.[21] In liquids, the anisotropy values range from 0.4 at $r(0)$ to 0.0 at $r(\infty)$ because rotational alignment is relaxed by collisions. Table 1 shows the expected values at time zero and at time infinity for each detection direction for gas-phase experiments. Differences among the different detection geometries are significant and well above signal-to-noise ratios of most URA measurements. Having identified the type of collection in the experiment, one can make quantitative URA measurements.

IV. Results and Discussion

Molecular iodine is one of the most extensively studied molecules by time-resolved methods (see refs 7 and 22−27 for example). Figure 1b illustrates the spectroscopic transitions involved in this experiment. Excitations resulting from the pump and probe beams are one photon, parallel transitions and only signal propagating at a right angle (X-direction) to the lasers is collected. The formulas applicable for this case are shown in Table 1 (column B). In Figure 3 we present experimental I_2 time-resolved measurements ($I_\parallel$ and $I_\perp$) for 550/311(340) and 622/311(340).

The transients used for the URA measurements were obtained with low-intensity laser beams to avoid any saturation effects on the anisotropy measurement. Saturation effects on anisotropy measurements are explored in a separate paper.[28] Experimental URA measurements are presented in Figure 4 (scattered points) and were calculated according to eq 5 both with and without normalization of the data (to 2 (||) and 1.3 (⊥) at time infinity for X-detection). We observed that using normalized versus unnormalized data in the anisotropy calculation and fitting routine changes the results only slightly (±3% for the rotational population temperature). Equation 8 is used in the fitting program with B constants obtained from ref 7. The fits to the normalized data sets, with temperature as the only adjustable parameter, are shown in Figure 4 (solid line). The experimentally obtained $r(t)$ are devoid of isotropic components such as vibrational oscillations and closely reproduce the theoretical values for $r(0)$ and $r(\infty)$ accurately (0.4 and 0.13). The slight deviation from 0.4 for the 622/311(340) transient can be explained by the

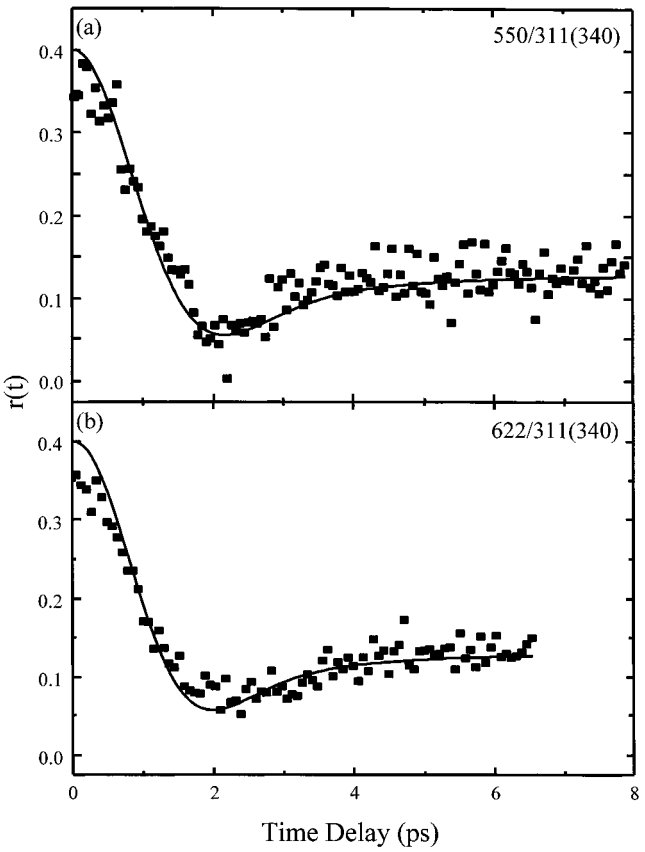

Figure 4. (a) URA measurements for 550/311(340) on I_2. (b) URA measurements for 622/311(340) on I_2. Rotational anisotropy values calculated from normalized experimental data and eq 5 are shown as the scattered points. Fits to these values using eq 8 are shown as the solid lines. The two measurements are best fit by thermal distributions of 294 ± 12 and 289 ± 12 K, respectively. Note that temperature is the only adjustable parameter.

contribution of a perpendicular transition to a repulsive state by the pump.[28] In addition, the fits reflect thermal populations of 294 ± 12 (550/311(340)) and 289 ± 12 K (622/311(340)) which correspond well with the temperature in the laboratory, 294 ± 3 K. Our results quantitatively reproduce the theory for unidirectional signal detection (*X*-direction). The equations in Table 1 provide the tools to properly analyze URA measurements given a particular experimental detection geometry.

Acknowledgment. Funding for this project comes from Grant No. CHE-9812584 of the National Science Foundation. M.D. is a Lucille and David Packard Science and Engineering Fellow and an Alfred P. Sloan Research Fellow. Additional funding for this project comes from a Camille Dreyfus Teacher-Scholar Award. E.J.B. is supported by a National Science Foundation Graduate Fellowship.

References and Notes

(1) *Femtochemistry*; Zewail, A. H., Ed.; World Scientific: Singapore, 1994; Vol. I and II.
(2) *Femtosecond Chemistry*; Manz, J., Woste, L., Eds.; Verlag Chemie GmbH: Weinheim, 1995; Vol. I and II.
(3) *Femtochemistry: Ultrafast Chemical and Physical Processes in Molecular Systems*; Chergui, M., Ed.; World Scientific: Singapore, 1996.
(4) Femtochemistry 97. *J. Phys. Chem.* **1998**, *102*, 4021 (Special Issue on Femtochemistry).
(5) Zewail, A. H. *J. Chem. Soc., Faraday Trans. 2* **1989**, *85*, 1221.
(6) Dantus, M.; Bowman, R. M.; Baskin, J. S.; Zewail, A. H. *Chem. Phys. Lett.* **1989**, *159*, 406.
(7) Gruebele, M.; Roberts, G.; Dantus, M.; Bowman, R. M.; Zewail, A. H. *Chem. Phys. Lett.* **1990**, *166*, 459.
(8) Spenser, J.; Baskin, J. S.; Zewail, A. H. *J. Phys. Chem.* **1994**, *98*, 3337.
(9) Baskin, J. S.; Zewail, A. H. *J. Phys. Chem.* **1994**, *98*, 3337 and references therein.
(10) Zhang, Q.; Marvet, U.; Dantus, M. *Faraday Discuss.* **1997**, *108*, 63.
(11) Zhang, Q.; Marvet, U.; Dantus, M. *J. Chem. Phys.* **1998**, *109*, 4428.
(12) Felker, P. M.; Baskin, J. S.; Zewail, A. H. *J. Phys. Chem.* **1986**, *90*, 724.
(13) Felker, P. M.; Zewail, A. H. *J. Chem. Phys.* **1987**, *86*, 2460.
(14) Heather, R.; Metiu, H. *Chem. Phys. Lett.* **1989**, *157*, 505.
(15) Felker, P. M. *J. Phys. Chem.* **1992**, *96*, 7844; Kaziska, A. J.; Shchuka, M. I.; Topp, M. R. *Chem. Phys. Lett.* **1991**, *183*, 52; Troxler, T.; Smith, P. G.; Topp, M. R. *Chem. Phys. Lett.* **1993**, *211*, 371.
(16) Felker, P. M.; Zewail, A. H. Molecular Structures from Ultrafast Coherence Spectroscopy. In *Femtosecond Chemistry*; Manz, J., Woste, L., Eds.; Verlag Chemie GmbH: Weinheim, 1995.
(17) Zare, R. N. *Mol. Photochem.* **1972**, *4*, 1.
(18) Gordon, R. G. *J. Chem. Phys.* **1966**, *45*, 1643.
(19) Marvet, U.; Zhang, Q.; Brown, E. J.; Dantus, M. *J. Chem. Phys.* **1998**, *109*, 4415.
(20) http://www.cem.msu.edu/~dantus/rotanis_simul.html.
(21) Baskin, J. S.; Gupta, M.; Chachisvilis, M.; Zewail, A. H. *Chem. Phys. Lett.* **1997**, *275*, 437.
(22) Bowman, R. M.; Dantus, M.; Zewail, A. H. *Chem. Phys. Lett.* **1989**, *161*, 297.
(23) Dantus, M.; Bowman, R. M.; Zewail, A. H. *Nature* **1990**, *343*, 737.
(24) Fischer, I.; Vrakking, M. J. J.; Villeneuve, D. M.; Stolow, A. *Chem. Phys.* **1996**, *207*, 331.
(25) Sarkisov, O. M.; Gostev, F. E.; Lozovoy, V. V.; Sviridenkov, E. A.; Titov, A. A.; Tovbin, D. G.; Umanskii, S. Y. *Russ. Chem. Bull.* **1996**, *45*, 553.
(26) Lozovoy, V. V.; Antipin, S. A.; Gostev, F. E.; Titov, A. A.; Tovbin, D. G.; Sarkisov, O. M.; Vetchinkin, A. S.; Umanskii, S. Y. *Chem. Phys. Lett.* **1998**, *284*, 221.
(27) Yakovlev, V. V.; Bardeen, C. J.; Che, J. W.; Cao, J. S.; Wilson, K. R. *J. Chem. Phys.* **1998**, *108*, 2309.
(28) Brown, E. J.; Pastirk, I.; Dantus, M. Manuscript in preparation.